

Conjugate Heat Transfer in an Annulus with Porous Medium Fixed Between Solids

Irfan Anjum Badruddin¹ · Salman Ahmed N. J.² ·
Abdullah A. A. Al-Rashed³ · N. Nik-Ghazali¹ · Mohammed Jameel⁴ ·
Sarfraz Kamangar¹ · H. M. T. Khaleed⁵ · T. M. Yunus Khan^{1,6}

Received: 26 December 2014 / Accepted: 13 June 2015 / Published online: 11 July 2015
© Springer Science+Business Media Dordrecht 2015

Abstract Conjugate heat transfer is an important area of research which has been in demand due to its applications related to various scientific and engineering fields. The current research is focused to study the heat transfer in a porous medium sandwiched between two solid walls of an annular vertical cylinder. The prime focus of the current study was to evaluate the effect of solid wall thickness, the influence of variable wall thickness at inner and the outer radius, the conductivity ratio and the solid wall conductivity ratio on the heat transfer characteristics of the porous medium. The surface at inner and outer radii of the annulus is maintained isothermally at T_h and T_∞ such that $T_h > T_\infty$. The governing partial differential equations for the conjugate heat transfer in porous medium and that of solid walls are converted into a set of algebraic equations with the help of finite element method and then solved simultaneously to predict the temperature variation in the solid wall as well as the porous region of the annular domain.

Keywords Porous media · Conjugate · Annulus · FEM · Conductivity ratio

✉ Irfan Anjum Badruddin
Irfan_magami@Rediffmail.com

¹ Department of Mechanical Engineering, University of Malaya, Kuala Lumpur 50603, Malaysia

² Faculty of Engineering and Technology, Multimedia University, Bukit Beruang, Malacca 75450, Malaysia

³ Public Authority for Applied Education and Training, Industrial Training Institute, Kuwait 13092, Kuwait

⁴ Department of Civil Engineering, University of Malaya, Kuala Lumpur 50603, Malaysia

⁵ Department of Mechanical Engineering, Faculty of Engineering, Islamic University, Madinah Munawwarra, Kingdom of Saudi Arabia

⁶ Department of Mechanical Engineering, BVB College of Engineering and Technology, Hubli 580031, India

List of symbols

H	Height of cylinder (m)
L	$r_o - r_i$ (m)
Ar	Aspect ratio = H/L
c_p	Specific heat (J/kg °C)
DL	Thickness ratio of inner solid $(r_{sp1} - r_i)/(r_o - r_i)$
DR	Thickness ratio of outer solid $(r_o - r_{sp2})/(r_o - r_i)$
g	Gravitational acceleration (m/s ²)
k	Thermal conductivity (W/m °C)
K	Permeability of the porous medium (m ²)
Kr	Thermal conductivity ratio = k_{s1}/k_p
Kr_o	Thermal conductivity ratio = k_{s2}/k_p
Krs	Thermal conductivity ratio of two solids k_{s1}/k_{s2}
\overline{Nu}	Average Nusselt number
r, z	Cylindrical coordinates (m)
\bar{r}, \bar{z}	Non-dimensional coordinates
Ra	Rayleigh number
Rr	Radius ratio = $(r_o - r_i)/r_i$
T, \bar{T}	Dimensional (°C) and non-dimensional temperature, respectively
u, w	Velocity in r and z directions, respectively (m/s)

Greek symbols

α	Thermal diffusivity (m ² /s)
β	Coefficient of thermal expansion (1/°C)
ρ	Density (kg/m ³)
ν	Coefficient of kinematic viscosity
ϕ	Porosity
$\Psi,$	Stream function
$\bar{\psi}$	Non-dimensional stream function

Subscripts

h	Hot
∞	Conditions at outer radius
i	Inner
o	Outer
p	Porous
s	Solid
sp	Solid–Porous interface

1 Introduction

The study of heat transfer in porous medium has attracted the attention of many researchers over the years. The prime reason for this interest can be directly linked with the fact that the

porous medium is involved in plenty of applications covering a vast range of scientific and engineering disciplines. Some of the examples of porous medium application can be found in the processes of heat extraction from geothermal sources, heat removal from nuclear reactor, heat exchangers, electronic components, solar energy storage technology, exothermic reactions in packed bed reactors, storage of grains, food processing, high-performance insulation for energy-efficient buildings, and the spread of pollutants underground to name but few. The deep insight and further applications of porous medium can be found in the well-documented books such as [Nield and Bejan \(2006\)](#), [Pop and Ingham \(2001\)](#), [Vafai \(2000\)](#). The phenomenon of natural convective heat transfer inside the porous medium has been investigated and documented in great details. Natural convection in porous medium refers to the condition when specific segment of the medium, generally boundaries, is subjected to differential heating which in turn creates a density difference between warm and cold fluid of medium, thus setting the fluid into motion. The moving fluid carries certain amount of heat alongside its motion making the heat transfer a complex phenomenon. The study carried out emphasizing the analyses of natural convection in different geometries fixed with porous medium witnesses the research interest exhibited in this area ([Salman et al. 2009](#); [Badruddin et al. 2006a, b, 2007a, b](#)). The heat transfer in porous medium is affected by many factors, and one of them is the case when solid wall having certain thickness is present alongside the porous medium. The presence of the solid wall affects the heat flow pattern inside the porous medium. This happens because of the fact that the boundary conditions are generally known at outer boundaries of the whole solid–porous system, but no information is available at the meeting point of solid and the porous region which can be termed as solid–porous interface. Thus, the heat transfer in the porous medium is dictated by the solid wall characteristics. This particular case when heat flow pattern is affected due to the presence of solid wall is referred to as conjugate heat transfer. The mathematical modeling of conjugate heat transfer requires an additional equation describing the heat transfer inside the solid wall apart from the usual momentum and energy equations of the porous region. There is relatively scarcity of literature pertaining to the conjugate heat transfer as compared to the heat transfer in porous medium without solid wall. There are various physical and geometrical parameters which affect the conjugate heat transfer rate, and in case of condensation process involving porous medium, the ratio of thermal resistance between the film condensation and the solid plate has great influence on determining the heat transfer characteristics of solid porous domain ([Char and Lin 2001](#)). It is established that the presence of a solid strip with heat generation can modify the temperature profile substantially in the porous medium ([Mendez et al. 2002](#)). It is reported that the reduction in aspect ratio by 25 % in a horizontal plate kept below the porous medium leads to 30–45 % reduction in temperature rise in the solid plate for Rayleigh number ranging from 1 to 1000 ([Vaszi et al. 2001](#)), and the plate thickness plays an important role in boundary layer formation ([Vaszi et al. 2002](#)). It is also noticed that in case of a solid cylindrical fin in porous medium, the local heat transfer coefficient and the local heat flux show a more gradual drop along the rounded tip as the aspect ratio of the fin becomes larger ([Vaszi et al. 2004](#)). In case of a horizontal solid strip dividing two porous media, the heat transfer rate is found to be stronger when the hot porous medium is below the strip than the other way round ([Higuera 1991](#)). The conjugate heat transfer in various shapes of porous media is reported in the literature which includes a semi-infinite porous medium adjacent to solid wall ([Pop and Merkin 1995](#)), bidisperse porous channel ([Nield and Kuznetsov 2004](#)), porous channel ([Shohel and Roydon 2005](#)), square cavity fixed with solid wall on the left side of the cavity ([Abdalla et al. 2008](#); [Saeid 2007a](#); [Baytaş et al. 2001](#); [Saleh and Hashim 2012](#)), square cavity embedded with a small solid heat source at the bottom surface of the cavity ([Aleshkova and Sheremet 2010](#)), vertical slender hollow cylinder ([Pop and Na 2000](#);

Ahmet Kaya 2011), and vertical cylinder with solid at inner radius (Salman et al. 2014). Apart from the above-mentioned cases, a porous cavity sandwiched between two solids has also been reported (Saeid 2007b; Alhashash et al. 2013). In this particular case, two solid walls having equal thickness and thermal conductivities are placed at left and right side of porous medium with boundary conditions applied at the solids walls. It is noticed that the conjugate heat transfer in an annular vertical cylinder having unequal thickness and thermal conductivities is not reported thus far to the best of author's knowledge. The annular porous medium sandwiched between inner and outer solids can be used in refineries and exhaust chimney where the hollow portion of the cylinder could be carrying the hot fluid and the solid-porous-solid could be acting as a composite wall.

2 Mathematical Model

The schematic representation of the physical model showing the conjugate heat transfer in an annular porous annulus along with the coordinate system is depicted in Fig. 1. The coordinate system is chosen in such a way that the r - and z -axes point toward the radial and vertical directions respectively of the annulus. Since this is a conjugate problem, a solid wall with finite thickness exists at the inner and outer radii of the annulus. The porous medium is sandwiched between these two solid walls. The solid wall thickness is defined as a fraction of the total thickness of the annulus between inner and outer radii. DL and DR refer to the fraction of solid wall at inner and outer surfaces, respectively. The conductivity ratio Kr indicates the ratio of thermal conductivity between inner solid to porous medium where as solid conductivity ratio Krs is the ratio of inner to outer wall thermal conductivity. The inner surface of the annulus is heated to constant temperature T_h , and the outer surface is maintained at constant temperature T_∞ such that $T_h > T_\infty$.

The following assumptions are applied

- The fluid obeys Darcy law.
- The convective fluid and the porous medium are in local thermal equilibrium.
- There is no phase change of fluid in the medium.
- The properties of the solid, fluid, and those of the porous medium are homogeneous
- Fluid properties are constant except the variation in density with temperature.

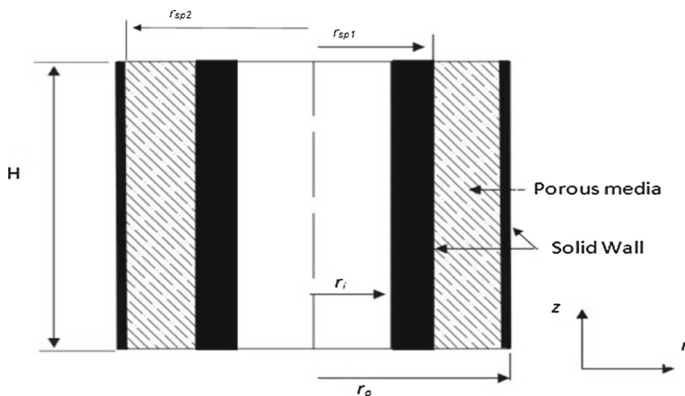


Fig. 1 Schematic of the physical model

The equations which dictate the heat and fluid flow in the porous solid regions of the domain are given by:

For porous region

$$\frac{\partial(ru)}{\partial r} + \frac{\partial(rw)}{\partial z} = 0 \tag{1}$$

$$\frac{\partial w}{\partial r} - \frac{\partial u}{\partial z} = \frac{gK\beta}{\nu} \frac{\partial T}{\partial r} \tag{2}$$

$$u \frac{\partial T_p}{\partial r} + w \frac{\partial T_p}{\partial z} = \frac{1}{r} \frac{\partial}{\partial r} \left(r \frac{\partial T_p}{\partial r} \right) + \frac{\partial^2 T_p}{\partial z^2} \tag{3}$$

For solid wall:

$$\frac{1}{r} \frac{\partial}{\partial r} \left(r \frac{\partial T_s}{\partial r} \right) + \frac{\partial^2 T_s}{\partial z^2} = 0 \tag{4}$$

Subjected to boundary conditions:

$$\text{at } r = r_i, \quad T_{s1} = T_h \tag{5a}$$

$$\text{at } r = r_o, \quad T_{s2} = T_\infty \tag{5b}$$

Since there is no heat storage in the medium, the following condition at solid–porous interface has to be satisfied

$$\text{at } r = r_{sp1} \quad u = 0 \quad T_{s1} = T_p \quad k_{si} \frac{\partial T_{s1}}{\partial r} = k_p \frac{\partial T_p}{\partial r} \tag{5c}$$

$$\text{at } r = r_{sp2} \quad u = 0 \quad T_p = T_{s2} \quad k_p \frac{\partial T_p}{\partial r} = k_{s2} \frac{\partial T_{s2}}{\partial r} \tag{5d}$$

The continuity Eq. (1) can be satisfied automatically by introducing the stream function ψ as:

$$u = -\frac{1}{r} \frac{\partial \psi}{\partial z} \tag{6a}$$

$$w = \frac{1}{r} \frac{\partial \psi}{\partial r} \tag{6b}$$

The following parameters have been used for non-dimensionalisation of the governing equations.

$$\bar{r} = \frac{r}{L}, \quad \bar{z} = \frac{z}{L}, \quad \bar{\psi} = \frac{\psi}{\alpha \varphi L}, \quad \bar{T} = \frac{(T - T_\infty)}{(T_h - T_\infty)}$$

$$Ra = \frac{g\beta \Delta T K L}{\nu \alpha_f} \tag{7}$$

Substitution of Eqs. (6)–(7) into Eqs. (2)–(4) results in:

$$\frac{\partial^2 \bar{\psi}}{\partial \bar{z}^2} + \bar{r} \frac{\partial}{\partial \bar{r}} \left(\frac{1}{\bar{r}} \frac{\partial \bar{\psi}}{\partial \bar{r}} \right) = \bar{r} Ra \frac{\partial \bar{T}_f}{\partial \bar{r}} \tag{8}$$

$$\frac{1}{\bar{r}} \left[\frac{\partial \bar{\psi}}{\partial \bar{r}} \frac{\partial \bar{T}_p}{\partial \bar{z}} - \frac{\partial \bar{\psi}}{\partial \bar{z}} \frac{\partial \bar{T}_p}{\partial \bar{r}} \right] = \frac{1}{\bar{r}} \frac{\partial}{\partial \bar{r}} \left(\bar{r} \frac{\partial \bar{T}_p}{\partial \bar{r}} \right) + \frac{\partial^2 \bar{T}_p}{\partial \bar{z}^2} \tag{9}$$

$$\frac{1}{\bar{r}} \frac{\partial}{\partial \bar{r}} \left(\bar{r} \frac{\partial \bar{T}_s}{\partial \bar{r}} \right) + \frac{\partial^2 \bar{T}_s}{\partial \bar{z}^2} = 0 \tag{10}$$

The boundary conditions take the form as:

$$\text{at } \bar{r} = r_i \quad \bar{T}_{s1} = 1 \tag{11a}$$

$$\text{at } \bar{r} = r_o \quad \bar{T}_{s2} = 0 \tag{11b}$$

$$\text{at } \bar{r} = r_{sp1} \quad \bar{\psi} = 0, \quad \bar{T}_{s1} = \bar{T}_p \quad Kr \frac{\partial \bar{T}_{s1}}{\partial \bar{r}} = \frac{\partial \bar{T}_p}{\partial \bar{r}} \tag{11c}$$

$$\text{at } \bar{r} = r_{sp2} \quad \bar{\psi} = 0, \quad \bar{T}_p = \bar{T}_{s2} \quad \frac{\partial \bar{T}_p}{\partial \bar{r}} = Kr_o \frac{\partial \bar{T}_{s2}}{\partial \bar{r}} \tag{12}$$

The Nusselt number is calculated using following expressions:

$$\bar{N}u = -\frac{1}{\bar{z}} \int_0^{\bar{z}} \left(\frac{\partial \bar{T}_p}{\partial \bar{r}} \right)_{\bar{r}=\bar{r}_{sp1}} d\bar{z} \tag{13}$$

3 Numerical Scheme

The equations that govern the heat transfer in solid section along with heat and fluid flow inside the porous medium are partial differential equations. These are coupled equations (Eqs. 8–10) having interdependency on each other. Any change in one equation affects the other equation and vice versa which makes them difficult to solve directly. Thus, these equations are to be solved simultaneously. Current numerical scheme is based on finite element method where Eqs. 8–10 are converted into algebraic form of equations with the help of Galerkin method (Segerland 1982; Lewis et al. 2004). The resultant set of algebraic equations is assembled into a global matrix for each of the Eqs. 8–10. It requires only a half of the domain to be modeled due to symmetric nature of the cylinder. A 3-noded triangular element is used to mesh the domain. The accuracy of finite element method generally depends on the number of elements being chosen to mesh the domain, and it increases with increase in number of elements until a point, thereafter the dependency becomes irrelevant. The geometry is meshed with sufficient number of elements to make sure that the results are not affected due to mesh size. Equations 8–10 are solved iteratively with tolerance level for $\bar{\psi}$ and \bar{T} are set as 10^{-7} and 10^{-5} , respectively. The tolerance level indicates the difference in the value of solution variable ($\bar{\psi}$ and \bar{T}) from its previous iteration for each of the nodes in the domain. The present methodology is validated with the previously published data by setting the solid wall thickness to zero that corresponds to vertical annular porous medium. The comparison is shown in Table 1 to illustrate that the current method is accurate enough to simulate the heat transfer behavior of problem under consideration.

Table 1 Comparison of results for different aspect ratio at $Ra = 100$, $Rr = 1$, $DL = DR = 0$

Aspect ratio	$\bar{N}u$			
	Prasad and Kulacki (1984)	Rajamani et al. (1995)	Nath and Satyamurthy (1985)	Present
3	3.70	3.868	3.81	3.8838
5	3.00	3.025	3.03	3.0638
8	2.35	2.403	2.45	2.4249

4 Results and Discussion

The problem under investigation is discussed for different physical and geometric parameters involved. Emphasis is given to the thickness of the solid walls at the inner and outer surfaces along with the conductivity ratio and solid conductivity ratio. Results are discussed in terms of Nusselt number at the solid–porous interface which is a measure of heat transfer from the solid wall to porous medium. Apart from Nusselt number, the temperature distribution at the solid–porous interface and the streamlines along with isothermal lines are presented for various physical and geometric parameters.

4.1 Temperature Profile

The boundary conditions of current problem are such that the inner and outer surfaces are maintained at T_h and T_∞ , respectively, which means that the heat has to travel from inner radius toward outer radius because of temperature difference in radial direction. The applied temperature exists on the left and right surfaces of the inner and outer solid walls. The heat transfer from solid wall to the porous medium and then from porous medium to outer solid depends on the temperature profile at the solid–porous interfaces. These profiles are in turn dependent on the solid wall thickness and the physical properties of walls. Since the domain includes two solid walls at inner and outer surfaces, it is important to know the temperature variations along the interfaces and the medium to judge the heat transfer characteristics of the whole domain.

Figures 2, 3 illustrate the effect of solid wall thickness on the temperature distribution at the inner and outer surface solid porous interfaces for $DL = 3.125, 6.25, 12.5, 25, 37.5$ & 50% at $DR = 6.25$ and 25% . Figures 2, 3, 4, and 5 correspond to $Ra = 200, Rr = 1, Ar = 5, Kr = 10, Krs = 2$. It is observed that the temperature of solid–porous interface at r_{sp1} is very close to that of the applied temperature T_h when the wall thickness DL is small but the temperature of interface at higher values of DL is substantially different from that of T_h . This

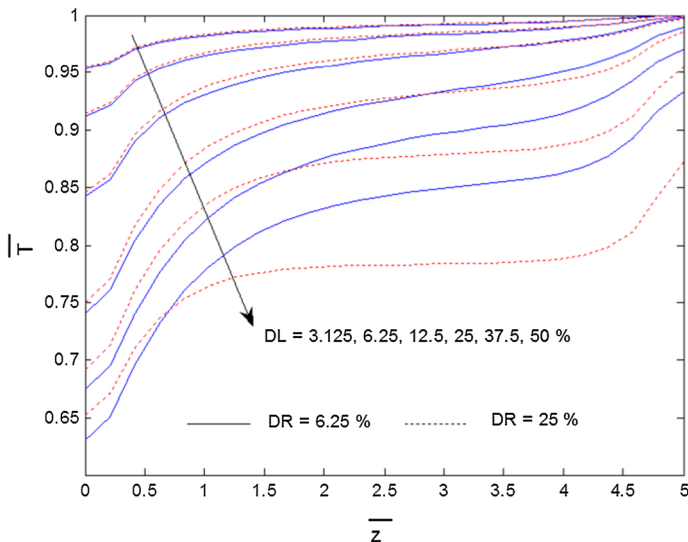


Fig. 2 Temperature along r_{sp1} when DL varies

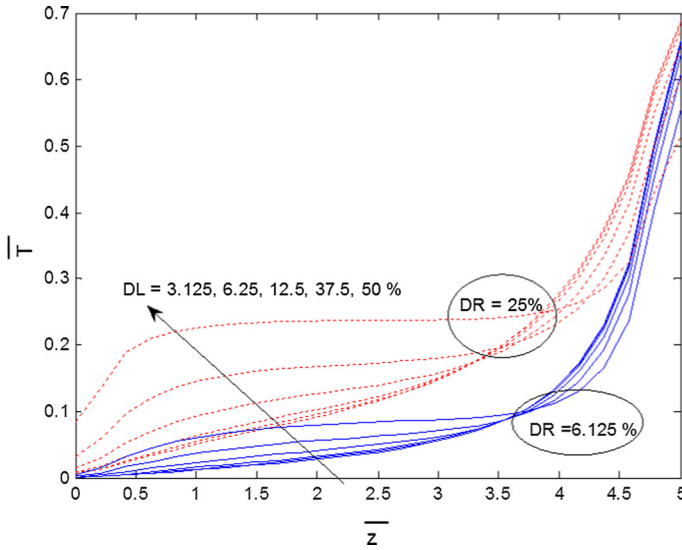


Fig. 3 Temperature along r_{sp2} when DL varies

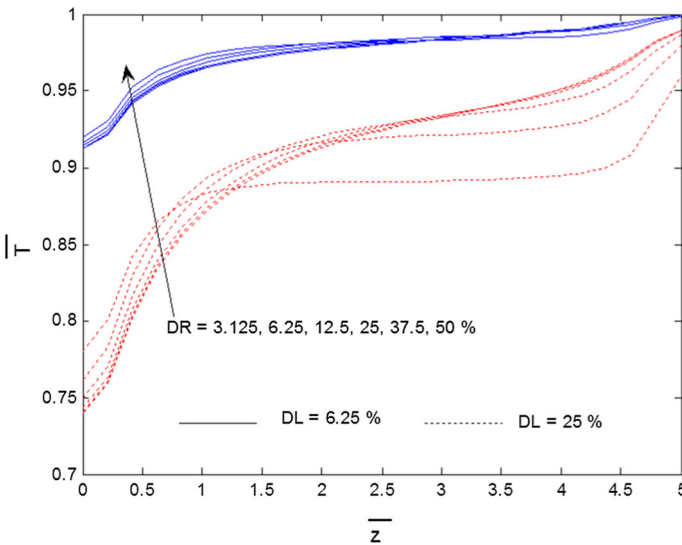


Fig. 4 Temperature along r_{sp2} when DR varies

is because the conduction resistance is low when left wall is thinner, thus facilitating the heat transfer in the inner solid that in turn increases the temperature across the inner solid. The temperature increases along the height of the cylinder. The variation in temperature at lower section of the cylinder is sharp as compared to other sections. The fluid movement near the interface creates sharp variation in temperature at the lower part of cylinder by absorbing heat near that region and then moving upwards where the already elevated fluid temperature does not allow further absorption of heat due to reduced temperature difference between fluid and the interface region at upper section of cylinder. The increase in the wall thickness at outer

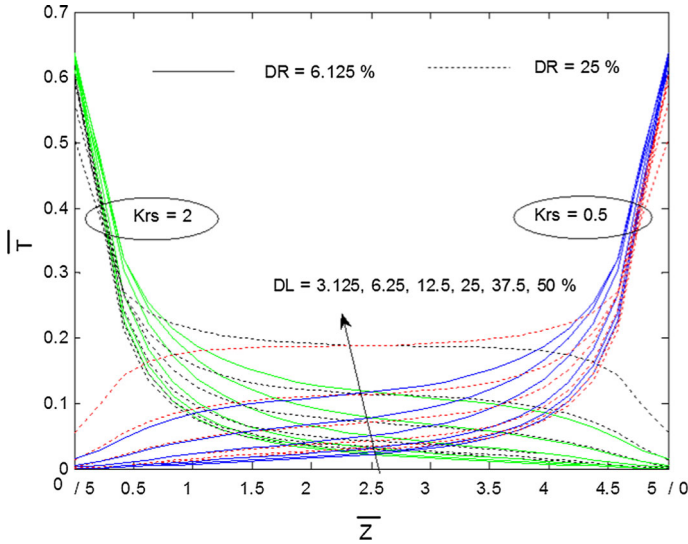


Fig. 5 Temperature along r_{sp2} when DR varies

surface, DR does not affect the interface temperature T_{sp1} for lower values of DL . However, the increase in DR reduces the interface temperature at upper section of cylinder for higher value of DL . The trend of temperature variation T_{sp2} for the porous–solid interface at outer surface as shown in Fig. 3 is completely different from that of inner surface temperature T_{sp1} . At r_{sp2} , the temperature increases gradually for most of the cylinder height until almost $Ar = 75\%$, and then, the increase is rapid for upper section. The fluid which has brought energy from r_{sp1} losses its most of the heat to the upper part of r_{sp2} ; thus, temperature in that region is higher as compared to the other sections of the interface r_{sp2} . At lower part of cylinder and given value of \bar{z} , the temperature is higher for higher inner wall thickness. This could be due to the reason that the fluid does not have enough strength to flow closer to lower part of r_{sp2} when width of porous medium is higher because of thinner DL . However, the fluid is forced to flow near to r_{sp2} when porous medium becomes thinner due to higher DL , resulting in better transfer of thermal energy in that vicinity of annulus. It is also observed that the temperature along r_{sp2} is higher for higher wall thickness at outer surface. The increased wall thickness DR is achieved at the cost of reduced porous thickness which in turn decreases thermal resistance along the depth of porous medium, thus increasing the temperature along r_{sp2} as depicted in Figs. 4, 5. It could be noted that Fig. 5 shows the temperature variation for two values of Krs which indicates the relative thermal conductivity of two solid walls. In Fig. 5, the height of the cylinder varies from left to right for $Krs = 2$ and right to left for $Krs = 0.5$. Figures 6 and 7 illustrate the effect of solid conductivity ratio Krs on interface temperature r_{sp1} and r_{sp2} , respectively. These figures correspond to the values $Ra = 300$, $Rr = 1$, $Ar = 5$, when both the solid walls have equal thickness of 6.25 and 25%. The temperature along r_{sp1} does not vary much for higher wall thickness. It is seen that the T_{sp1} is higher when the conductivity of left solid wall is higher than the solid wall at outer surface of cylinder leading to higher value of Krs , for a given value of porous medium thermal conductivity. It can be reasoned that the higher conductivity of inner solid facilitates greater heat transfer leading to increased temperature T_{sp1} . The effect of Krs reduces considerably when the porous conductivity is much lesser than the inner surface solid wall conductivity (higher Kr).

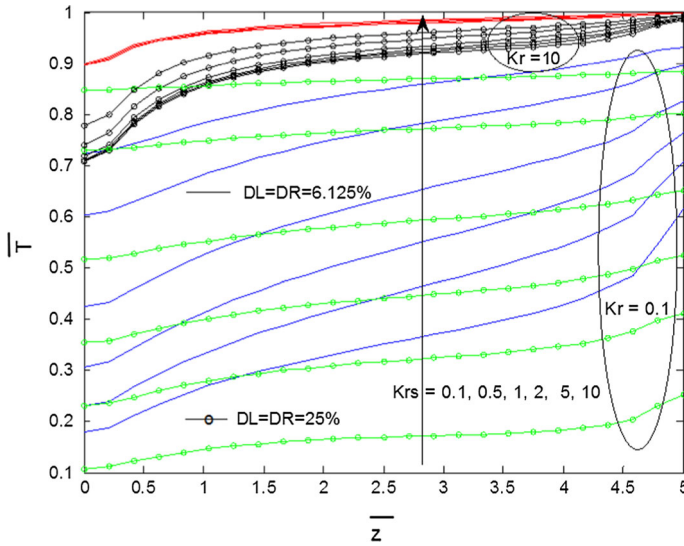


Fig. 6 Temperature along r_{sp1} when Krs varies

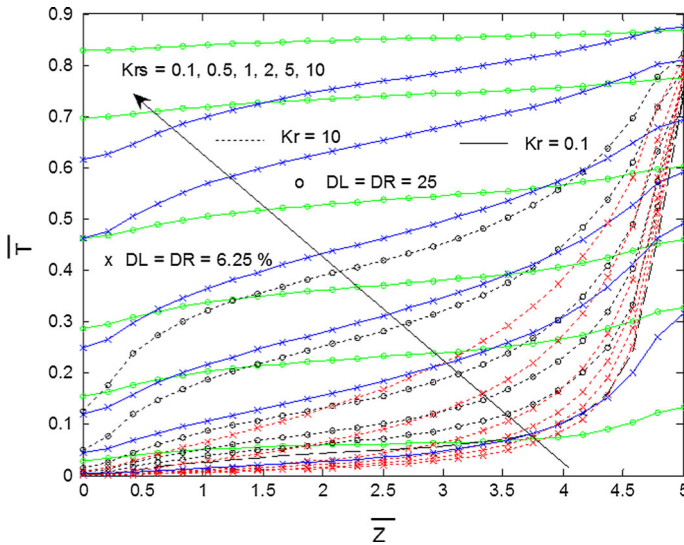


Fig. 7 Temperature along r_{sp2} when Krs varies

4.2 Streamlines and Isotherms

The fluid flow pattern and the temperature variation in the domain can be well described with the help of streamlines and the isothermal lines which basically represent the areas of constant values of stream function and the temperature. The effect of solid wall thickness variation when $DL = DR$ is shown in Fig. 8. This figure is obtained by setting $Ra = 200$, $Rr = 1$, $Ar = 5$, $Kr = 10$, $Krs = 5$. Isotherms are placed left and streamlines on right side of the figure for three values of inner and outer wall thickness. It is seen that the left solid wall

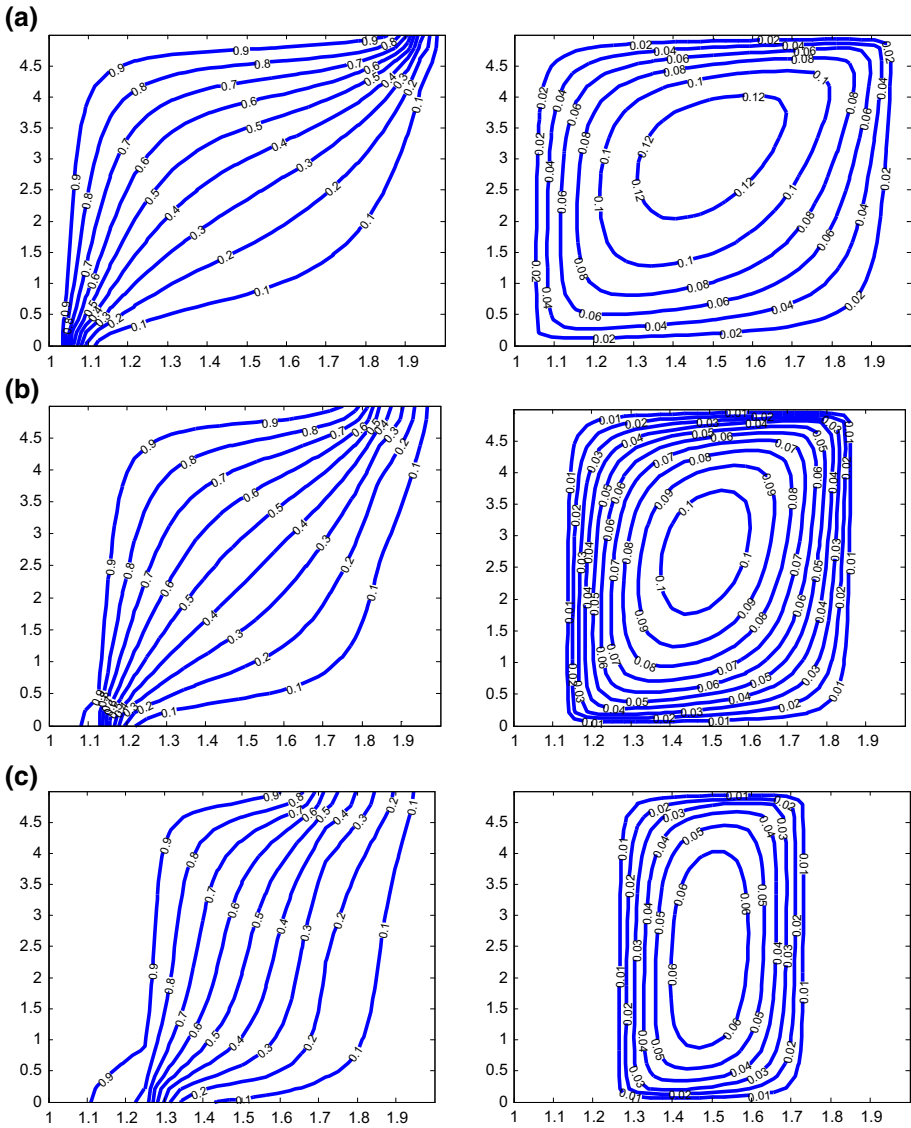


Fig. 8 Isotherms (left) , streamlines (right) for **a** $DL = DR = 6.25\%$, **b** $DL = DR = 12.5\%$, **c** $DL = DR = 25\%$ at $Ra = 200$, $Rr = 1$, $Ar = 5$, $Kr = 10$, $Krs = 5$

is occupied by high-temperature lines, indicating that higher amount of energy is transferred from inner radius to r_{sp1} because of high conductivity of the inner solid ($Kr = 10$). The outer solid is occupied by low-temperature isotherms because of low conductivity of outer solid. At low values of DL/DR , the fluid gains thermal energy at the lower left segment of cylinder and then moves toward the right upper segment losing its energy to outer surface before flowing back toward the left segment of cylinder, thus completing the cycle. The flow pattern is oval-shaped from lower left to upper right segment of the annulus. The increased wall thickness shifts the flow direction from being oval to near elliptical from bottom to top of the annulus.

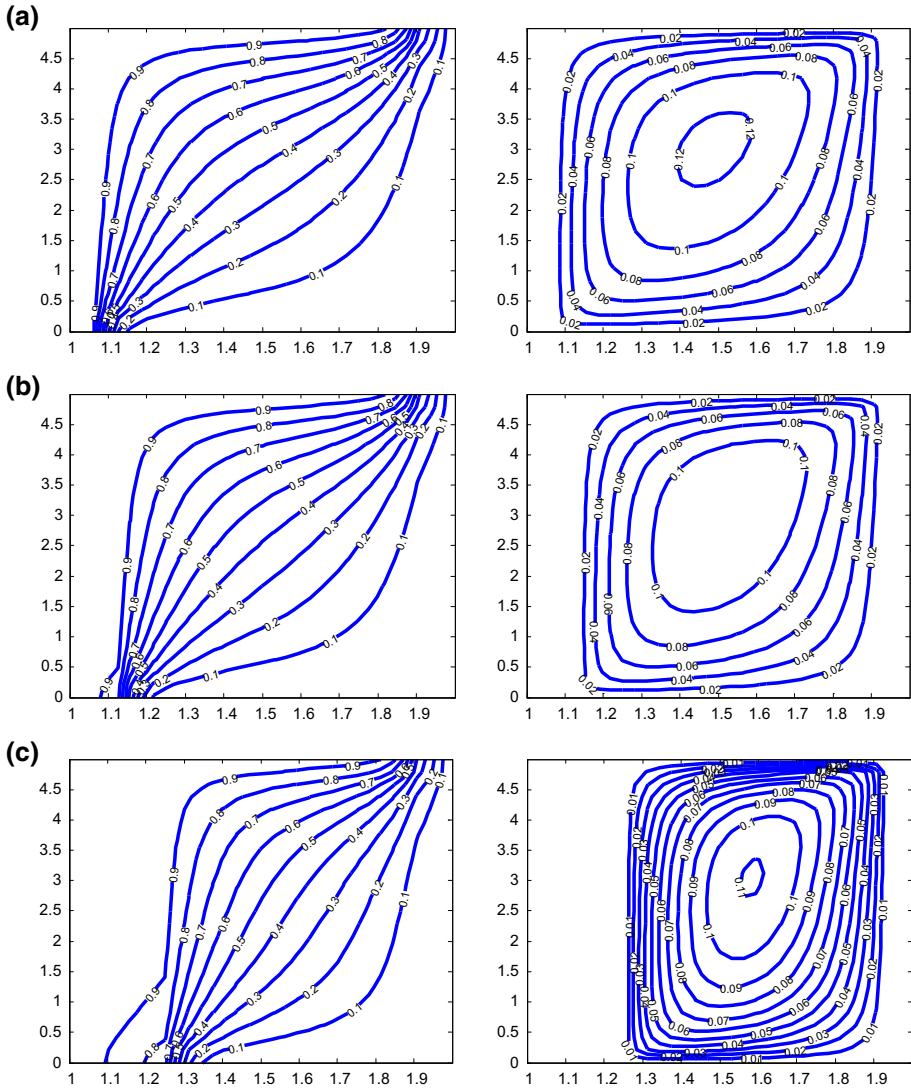


Fig. 9 Isotherms (left) , streamlines (right) for **a** $DL = 6.25\%$, **b** $DL = 12.5\%$, **c** $DL = 25\%$ at $Ra = 200$, $Rr = 1, Ar = 5, Kr = 10, Krs = 5, DR = 6.25\%$

Figure 9 indicates the effect of varying inner solid wall thickness by keeping the constant values $Ra = 200, Rr = 1, Ar = 5, Kr = 10, Krs = 5, DR = 6.25\%$. There is slight straightening of isotherms with increase in the wall thickness which indicates that the convection has reduced. This is further vindicated by reduction in the value of streamlines with increase in DL . The reduced stream function leads to reduction in the fluid velocity which in turn retards the heat transfer rate at the solid porous interface. The effect of varying the outer wall thickness is shown in Fig. 10 which is obtained at $Ra = 200, Rr = 1, Ar = 5, Kr = 10, Krs = 5, DL = 3.125\%$. It is obvious from Fig. 10 that the isotherms have considerably straightened when DR is varied from 6.25 to 50%. This reflects that the heat transfer due to

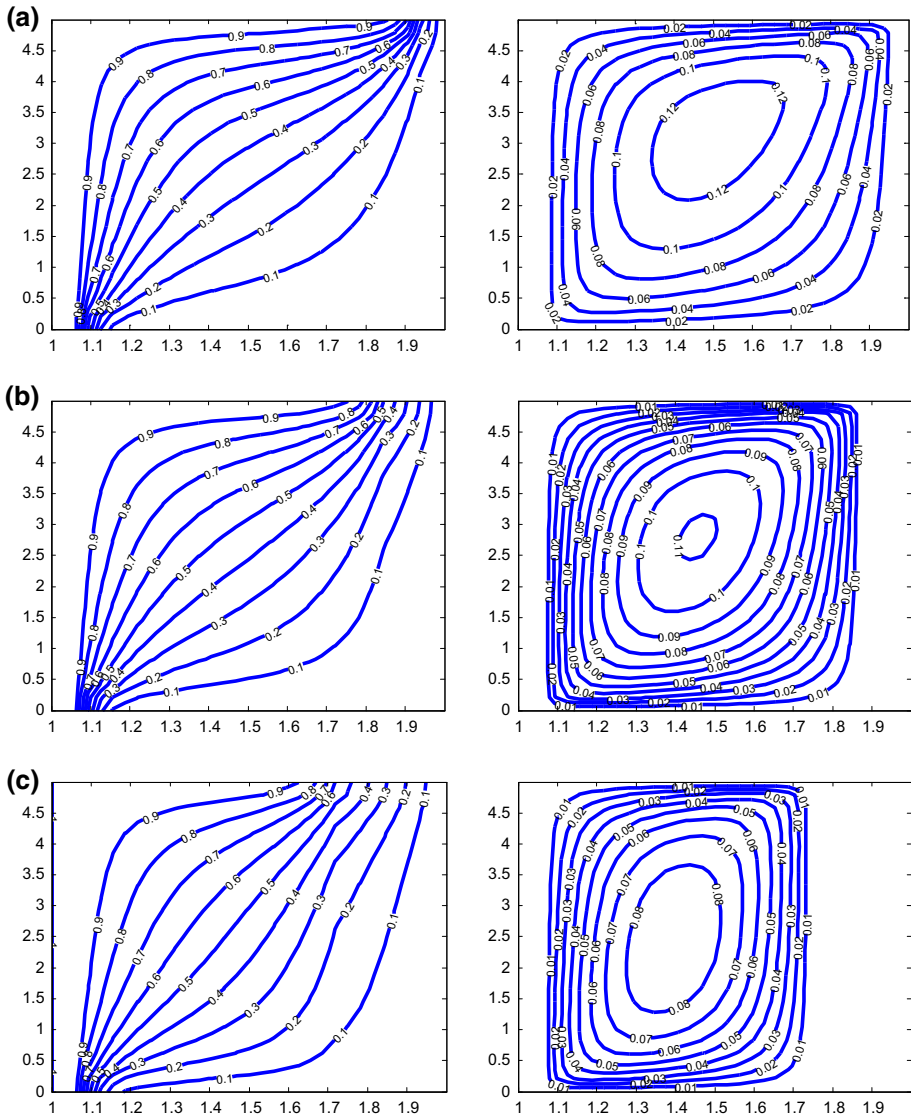


Fig. 10 Isotherms (left) , streamlines (right) for **a** $DR = 6.25\%$, **b** $DR = 12.5\%$, **c** $DR = 25\%$ at $Ra = 200$, $Rr = 1$, $Ar = 5$, $Kr = 10$, $Krs = 5$, $DL = 3.125\%$

convection reduces when DR is increased. The value of stream function reduces with increase in DR . Thus, it can be said that the increase in the either wall thickness reduces the fluid velocity inside the porous medium.

The effect of solid conductivity ratio on the streamline and isotherms is shown in Fig. 11. This figure belongs to $Ra = 200$, $Rr = 1$, $Ar = 5$, $Kr = 10$, $DL = 12.5\%$, $DR = 12.5\%$. The increase in solid conductivity ratio reduces the thermal gradient as indicated by spread out isotherms due to increase in Krs . The fluid velocity is reduced due to increase in Krs as indicated by streamlines.

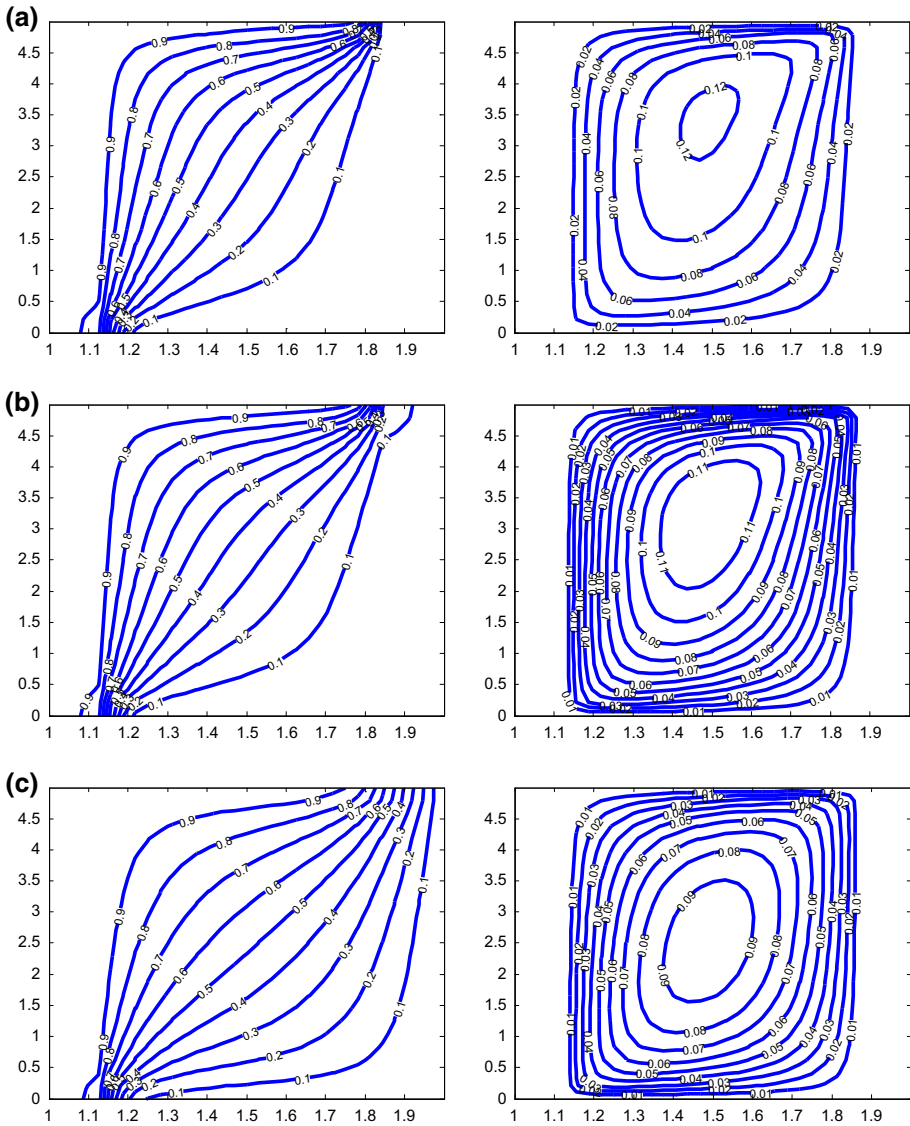


Fig. 11 Isotherms (left), streamlines (right) for **a** $Krs = 0.1$, **b** $Krs = 1$, **c** $Krs = 10$ at $Ra = 200$, $Rr = 1$, $Ar = 5$, $Kr = 10$, $DL = 12.5\%$, $DR = 12.5\%$

Figure 12 demonstrates the effect of variation in thermal conductivity ratio Kr on streamlines and isotherms. This figure is obtained by maintaining $Ra = 200$, $Rr = 1$, $Ar = 5$, $Krs = 10$, $DL = 12.5\%$, $DR = 12.5\%$. It is obvious from Fig. 12 that the fluid velocity increases with increase in thermal conductivity ratio. This can be attributed to the fact that the higher Kr is associated with increase in thermal conductivity of inner solid keeping the porous conductivity at constant value which in turn allows more heat to be transferred to porous medium leading to better fluid movement.

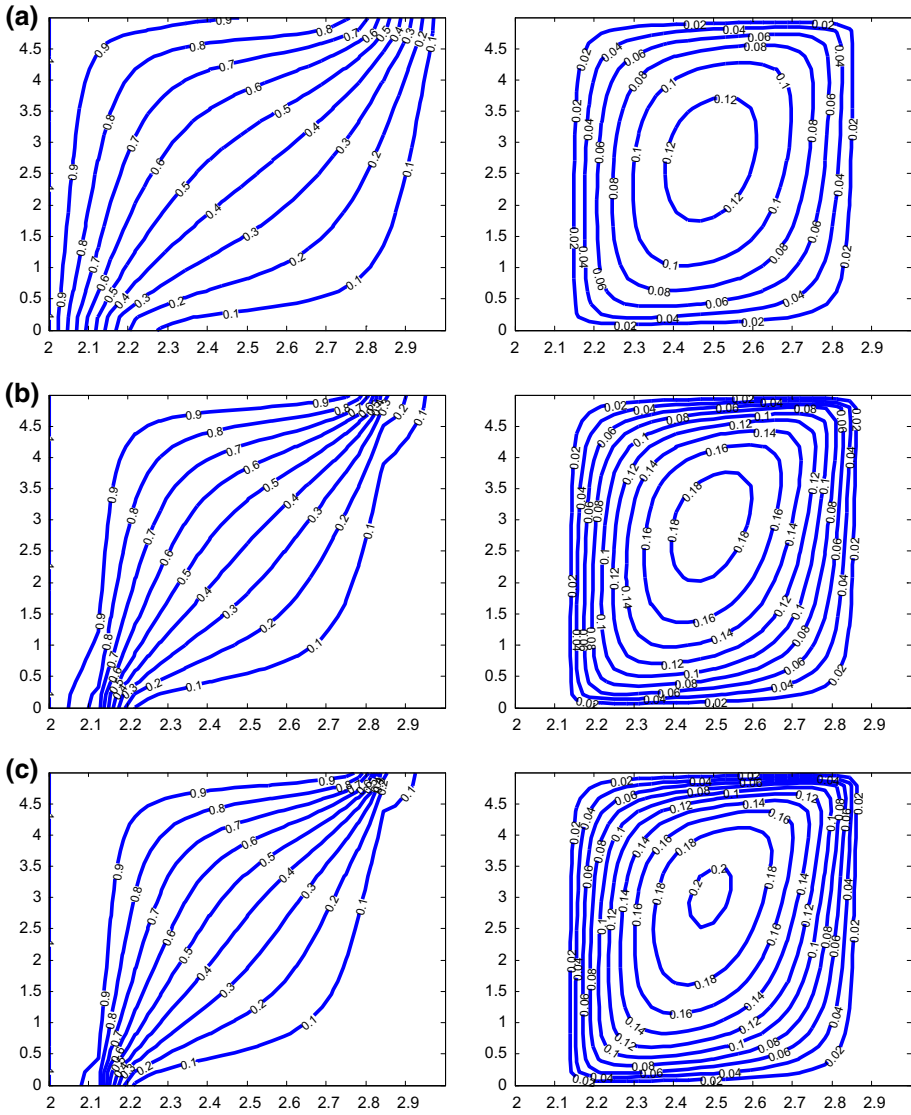


Fig. 12 Isotherms (left), streamlines (right) for **a** $Kr = 1$, **b** $Kr = 5$, **c** $Kr = 10$ at $Ra = 200$, $Rr = 1$, $Ar = 5$, $Krs = 10$, $DL = 12.5\%$, $DR = 12.5\%$

4.3 Heat Transfer in the Domain

The heat transfer from inner radius toward outer radius of the annular solid-porous-solid domain can be described with the help of Nusselt number. Nusselt number basically highlights the convective heat transfer relative to conduction. The following section discusses the variation in Nusselt number due to changes in various physical and geometric parameters. Figure 13 shows the average Nusselt number at r_{sp1} due to change in DL . This figure is obtained by setting $Ra = 200$, $Rr = 1$, $Ar = 5$, $Kr = 10$. It is observed that the average Nusselt number \bar{Nu} decreases with increase in the wall thickness DL for thin outer wall thickness.

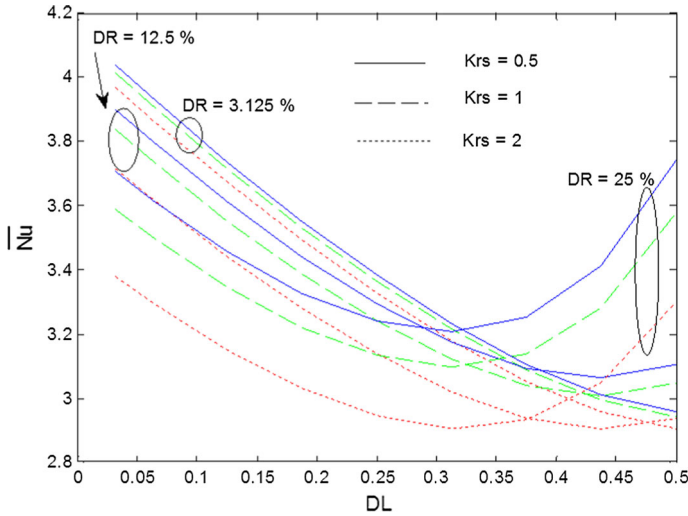


Fig. 13 \bar{Nu} variation with respect to DL

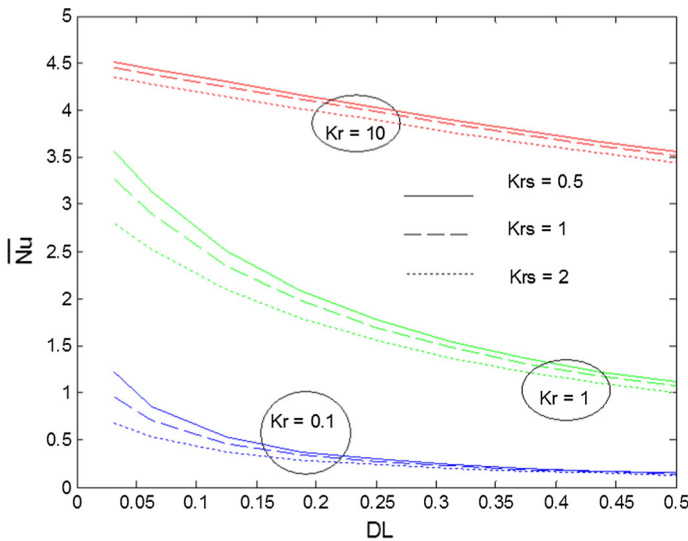


Fig. 14 \bar{Nu} variation with respect to DL for various thermal conductivity ratios

However, for thicker outer wall thickness, the \bar{Nu} initially decreases with respect to DL and then increases with further increase in DL . The decrease in \bar{Nu} with respect to increase in DL is a result of reduction in the T_{sp1} due to increased thermal resistance created by thickening solid wall at inner surface. However, the increase in the \bar{Nu} at higher outer wall thickness is associated with increased thermal gradient across r_{sp1} which offsets the effect of decreased interface temperature T_{sp1} . The increase in the conductivity ratio Kr increases the heat transfer rate as indicated by Fig. 14 that belongs to $Ra = 100, Rr = 1, Ar = 1, DR = 6.25$. The effect of Krs diminishes as the solid wall thickness DL increases. The \bar{Nu} variation is

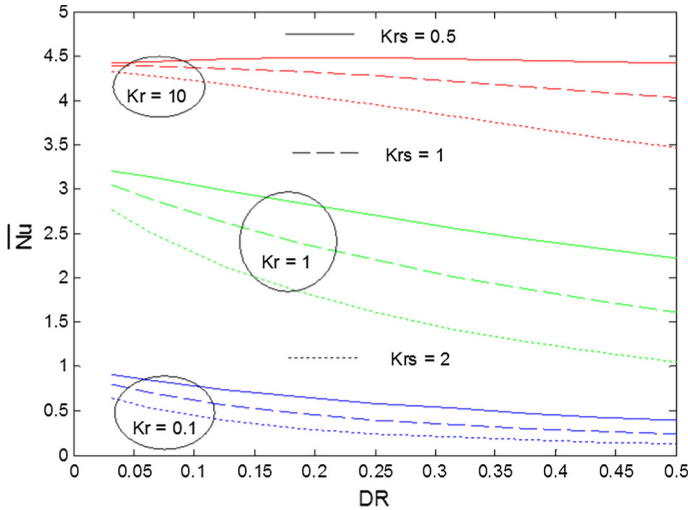


Fig. 15 \bar{Nu} variation with respect to DR

almost linear when the relative conductivity of inner solid is high compared to that of porous conductivity.

The effect of outer wall thickness DR on heat transfer rate is depicted in Fig. 15 which is obtained by setting $Ra = 100, Rr = 1, Ar = 1, DR = 6.25$. The Nusselt number decreases with increase in the DR . The variation in heat transfer with respect to change in DR is almost linear as shown in Fig. 15. The thermal conductivity ratio of inner and outer solids which is denoted by Krs plays an important role in determining the heat transfer characteristics inside the solid–porous–solid domain. The value $Krs > 1$ indicates that the conductivity of inner solid is higher than that of outer solid and vice versa for $Krs < 1$. The combination of different grades of aluminum at inner radius and steel at outer radii of annulus can have the $Krs \approx 10$. It is seen that the heat transfer rate decreases with increase in the Krs as illustrated by Fig. 16. The decrease in heat transfer with increase in Krs can be explained in a way that the increased solid conductivity ratio is associated with decrease in the thermal conductivity of outer solid. The decrease in the outer solid conductivity contributes to increase in the overall thermal resistance of porous–solid combination which in turn reduces the Nusselt number at r_{sp1} . It is worth mentioning that the increase in Krs is associated either with increase in k_{s1} or decrease in k_{s2} . If Kr is fixed as in case of Fig. 16, then the only way to increase Krs is by decreasing k_{s2} that leads to higher thermal resistance of the outer wall and thus the whole domain, resulting into decreased heat transfer rate as shown in Fig. 16. However, this decrease is negligible when the decrease in k_{s2} is counterbalanced by increase in porous conductivity (low Kr) or thinning of inner or outer wall resulting into low thermal resistance of overall domain. The increase in Krs is also associated with increase in the inner wall conductivity k_{s1} by keeping outer solid conductivity at constant value. In such condition, the overall thermal resistance of the whole domain decreases due to increase in k_{s1} that in turn increases Kr and heat transfer rate as shown in Fig. 16 ($Ra = 100, Rr = 1, Ar = 1$). The effect of Rayleigh number on Nusselt number is shown in Fig. 17 which is obtained at $DL = 12.5, DR = 12.5, Rr = 1, Ar = 10$. As expected, the heat transfer rate increases with increase in Rayleigh number. For a given value of Krs , the effect of Rayleigh number is higher when Kr is high. The high Rayleigh number and Kr lead to increased fluid energy and thus velocity which reflects in the form of increased Nusselt number.

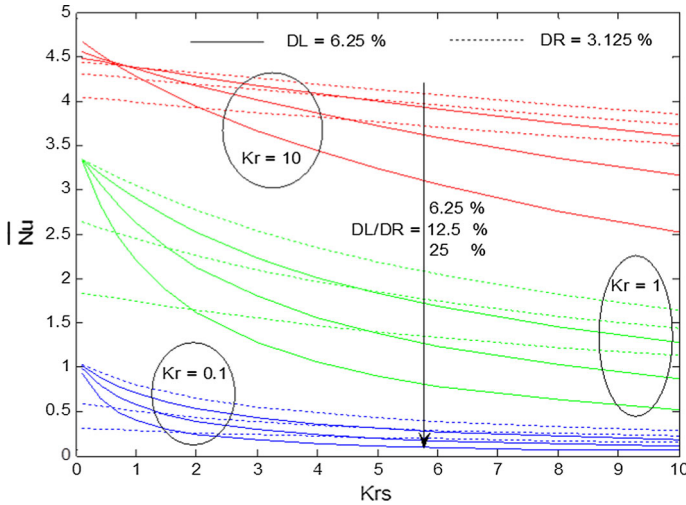


Fig. 16 \bar{Nu} variation with respect to Krs

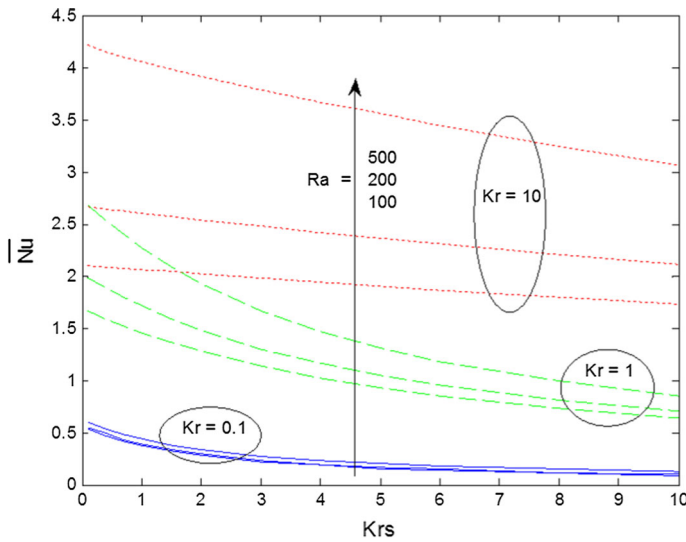


Fig. 17 Effect of Rayleigh number on \bar{Nu}

5 Conclusion

Conjugate heat transfer in an annular porous medium sandwiched between inner and outer solid walls is investigated with specific emphasis on the solid thickness and the conductivity ratio. Finite element method is used to solve the governing equations. It is found that there is not much temperature variation inside the inner solid when the wall thickness is small. The temperature at solid porous interface r_{sp1} increases along the height of the cylinder. At r_{sp2} , the temperature increases gradually for most of the cylinder height until almost $Ar = 75\%$ and then, the increase is rapid for upper section. It is also observed that the temperature along r_{sp2} is higher for higher wall thickness at outer surface. It is observed that the average

Nusselt number decreases with increase in the wall thickness DL for thin outer wall thickness. However, for thicker outer wall thickness, the $\bar{N}u$ initially decreases with respect to DL and then increases with further increase in DL . The increase in the conductivity ratio Kr increases the heat transfer rate. The effect of Krs diminishes as the solid wall thickness DL increases. It seems that the heat transfer rate decreases with increase in the Krs .

Acknowledgments The authors would like to thank University of Malaya for providing fund under the UMRG Grant No. RP006A-13AET.

References

- Abdalla, A.A., Khalil, K., Ioan, P.: Steady-state conjugate natural convection in a fluid-saturated porous cavity. Int. J. Heat Mass Transfer **51**(17–18), 4260–4275 (2008)
- Aleshkova, I.A., Sheremet, M.A.: Unsteady conjugate natural convection in a square enclosure filled with a porous medium. Int. J. Heat Mass Transfer **53**(23–24), 5308–5320 (2010)
- Ahmet, K.: Effects of buoyancy and conjugate heat transfer on non-Darcy mixed convection about a vertical slender hollow cylinder embedded in a porous medium with high porosity. Int. J. Heat Mass Transfer **54**(4), 31818–31825 (2011)
- Alhashash, A., Saleh, H., Hashim, I.: Conjugate natural convection in a porous enclosure sandwiched by finite walls under the influence of non-uniform heat generation and radiation. Transp. Porous Med. **99**, 453–465 (2013)
- Baytaş, A., Liaqat, C., Groşan, A., Pop, T.: Conjugate natural convection in a square porous cavity. Heat Mass Transfer **37**, 467–473 (2001)
- Badruddin, I.A., Zainal, Z.A., Narayana, A.P.A., Seetharamu, K.N.: Numerical analysis of convection conduction and radiation using a non-equilibrium model in a square porous cavity. Int. J. Therm. Sci. **46**(1), 20–29 (2007)
- Badruddin, I.A., Zainal, Z.A., Narayana, A.P.A., Seetharamu, K.N.: Heat transfer in porous cavity under the influence of radiation and viscous dissipation. Int. Commun. Heat Mass Transfer **33**, 491–499 (2006)
- Badruddin, I.A., Zainal, Z.A., Narayana, A.P.A., Seetharamu, K.N.: Thermal non-equilibrium modeling of heat transfer through vertical annulus embedded with porous medium. Int. J. Heat Mass Transfer **49**(25–26), 4955–4965 (2006)
- Badruddin, I.A., Zainal, Z.A., Zahid, A.K., Zulquernain, M.: Effect of viscous dissipation and radiation on natural convection in a porous medium embedded within vertical annulus. Int. J. Therm. Sci. **46**, 221–227 (2007)
- Char, M.L., Lin, J.D.: Conjugate film condensation and natural convection between two porous media separated by a vertical plate. In: 14 Acta Mechanica 9th. Springer, Berlin (2001)
- Higuera, F.J.: Conjugate natural convection heat transfer between two porous media separated by a horizontal wall. Int. J. Heat Mass Transfer **40**, 3157–3161 (1991)
- Lewis, R.W., Nithiaras, P., Seetharamu, K.N.: Fundamentals of the Finite Element Method for Heat and Fluid Flow. Wiley, Chichester (2004)
- Mendez, F., Trevino, C., Pop, I., Lenan, A.: Conjugate free convection along a thin vertical plate with internal non-uniform heat generation in porous medium. Int. J. Heat Mass Transfer **38**(13–14), 631–638 (2002)
- Nath, S.K., Satyamurthy, V.V.: Effect of aspect ratio and radius ratio on free convection heat transfer in a cylindrical annulus filled with porous media. HMT C16–85. In: Proceedings of 8th National Heat Mass Transfer Conference India. pp. 189–193 (1985)
- Nield, D.A., Bejan, A.: Convection in Porous Media, 3rd edn. Springer, New York (2006)
- Nield, D.A., Kuznetsov, A.V.: Forced convection in a bi-disperse porous medium channel: a conjugate problem. Int. J. Heat Mass Transfer **47**(24), 5375–5380 (2004)
- Pop, I., Ingham, D.B.: Convective Heat Transfer. Mathematical and Computational Modeling of Viscous Fluids and Porous Media. Pergamon, Oxford (2001)
- Pop, I., Merkin, J.H.: Conjugate free convection on vertical surfaces in a saturated porous medium. Fluid Dyn. Res. **16**, 71–86 (1995)
- Pop, I., Na, T.Y.: Conjugate free convection over a vertical slender hollow cylinder embedded in a porous medium. Heat Mass Transfer **36**, 375–379 (2000)
- Prasad, V., Kulacki, F.A.: Natural convection in a vertical porous annulus. Int. J. Heat Mass Transfer **27**, 207–219 (1984)
- Rajamani, R.C., Srinivas, C., Nithiarasu, P., Seetharamu, K.N.: Convective heat transfer in axisymmetric porous bodies. Int. J. Numer. Methods Heat Fluid Flow **5**, 829–837 (1995)

- Saeid, N.H.: Conjugate natural convection in a porous enclosure: effect of conduction in one of the vertical walls. *Int. J. Therm. Sci.* **46**(6), 531–539 (2007a)
- Saeid, N.H.: Conjugate natural convection in a vertical porous layer sandwiched by finite thickness walls. *Int. Commun. Heat Mass Transfer* **34**(2), 210–216 (2007b)
- Salman, A.N.J., Sarfaraz, K., Badruddin, I.A., Abdullah, A.A.A.A., Quadir, G.A., Khaleed, H.M.T., Khan, Y.T.M.: Conjugate heat transfer in porous annulus. *J. Porous Media* **17**(12), 1109–1119 (2014)
- Salman, A.N.J., Badruddin, I.A., Zainal, Z.A., Khaleed, H.M.T., Jeevan, K.: Heat transfer in a conical cylinder with porous medium. *Int. J. Heat Mass Transfer* **52**(13–14), 3070–3078 (2009)
- Saleh, H., Hashim, I.: Conjugate natural convection in a porous enclosure with non-uniform heat generation. *Transp. Porous Med.* **94**, 759–774 (2012)
- Segerland, L.J.: *Applied Finite Element Analysis*. Wiley, New York (1982)
- Shohel, M., Roydon, A.: Conjugate heat transfer inside a porous channel. *Heat Mass Transfer* **41**, 568–575 (2005)
- Vafai, K. (Ed). *Handbook of Porous Media*. Marcel Dekker, New York (2000)
- Vaszi, A.Z., Elliott, L., Ingham, D.B., Pop, I.: Conjugate free convection above a cooled finite horizontal flat plate embedded in a porous medium. *Int. Commun. Heat Mass Transfer* **28**, 703–712 (2001)
- Vaszi, A.Z., Elliott, L., Ingham, D.B., Pop, I.: Conjugate free convection above a heated finite horizontal flat plate embedded in a porous medium. *Int. J. Heat Mass Transfer* **45**, 2777–2795 (2002)
- Vaszi, A.Z., Elliott, L., Ingham, D.B., Pop, I.: Conjugate free convection from a vertical plate fin with a rounded tip embedded in a porous medium. *Int. J. Heat Mass Transfer* **47**, 2785–2794 (2004)